Soot Formation During Pyrolysis and Oxidation of Aliphatic and Aromatic Hydrocarbons in Shock Waves: Experiments and Detailed Kinetic Modeling

G.L. Agafonov, I.V. Bilera, Y.A. Kolbanovsky, V.N. Smirnov, A.M. Tereza, and P.A. Vlasov

Introduction

Our experimental and modeling study of soot formation during the pyrolysis of a number of aromatic (benzene, toluene, and ethylbenzene [1]) and saturated aliphatic hydrocarbons (methane, propane [2–4]) showed good agreement between the results of experiments and detailed kinetic modeling. However, certain difficulties were encountered in the kinetic simulation of soot formation in the pyrolysis of acetylene, a hydrocarbon with a triple bond. These difficulties have been overcome by introducing additional reaction channels of soot nucleation from hydrogenated polyyne-like fragments, in particular, diacetylene dimers. The experiments performed in [5] confirmed the possibility of the formation of high concentrations of diacetylene dimers in the reaction mixture.

The aim of this work was to perform experimental and kinetic modeling studies of soot formation in the pyrolysis and oxidation of various mixtures of aliphatic and aromatic hydrocarbons in argon behind reflected shock waves and to demonstrate the predictive capabilities of the modified kinetic model of soot formation.

G.L. Agafonov • V.N. Smirnov • A.M. Tereza
Semenov Institute of Chemical Physics, Russian Academy of Sciences, Kosygin Str. 4, 119991 Moscow, Russia

I.V. Bilera • Y.A. Kolbanovsky
Topchiev Institute of Petrochemical Synthesis, Russian Academy of Sciences, Leninskii Prospekt 29, 119991 Moscow, Russia

P.A. Vlasov (✉)
Semenov Institute of Chemical Physics, Russian Academy of Sciences, Kosygin Str. 4, 119991 Moscow, Russia

National Nuclear Research University "MEPhI", Kashirskoye Shosse 31, 115409 Moscow, Russia
e-mail: iz@chph.ras.ru

Results

The soot yield and temperature of soot particles were determined using a two-beam technique that enables to simultaneously measure the optical absorption and emission of soot particles. Details of the shock-tube setup were described elsewhere [3]. Figure 1 shows typical time histories of the absorption (1) and emission (2) signals after the arrival of the reflected shock wave front at the observation section, as well as the time evolution of the soot yield (3) and the soot particle temperature (4) obtained from signals (1) and (2) for the pyrolysis of a 5 % mixture of acetylene in argon under various conditions behind the reflected shock wave.

Experimentally measured dependences of the soot yield on the initial temperature of the test mixture behind the reflected shock wave for three different acetylene–argon mixtures are displayed in Fig. 2. These curves have a characteristic bell-like shape. As can be seen, the soot yield strongly depends on the initial concentration of acetylene in the test mixture. Figure 3 shows the deviation of the temperature of soot particles formed during the pyrolysis of acetylene–argon mixtures for a reaction time of 1 ms from the calculated initial temperature behind the reflected shock wave.

Taking into account that acetylene plays a key role in soot formation, that the pyrolysis and oxidation of virtually all hydrocarbons under fuel-rich conditions lead to the formation of high concentrations of acetylene, and that the role of acetylene as a building material in the surface growth of soot particles has been recognized for a long time, being beyond doubt, we performed the kinetic model validation for acetylene and diacetylene. The kinetic model was tested by a direct comparison of the experimentally measured [6, 7] and calculated product yields during diacetylene and acetylene pyrolysis and oxidation. The results are presented in Figs. 4 and 5. Three different $C_2H_2/H_2/Ar$ mixtures were investigated (Fig. 5): (a) 4.0 % C_2H_2 + 96 % Ar, (b) 2.5 % C_2H_2 + 97.5 % Ar, and

G. Ben-Dor et al. (eds.), *30th International Symposium on Shock Waves 1*, DOI 10.1007/978-3-319-46213-4_54

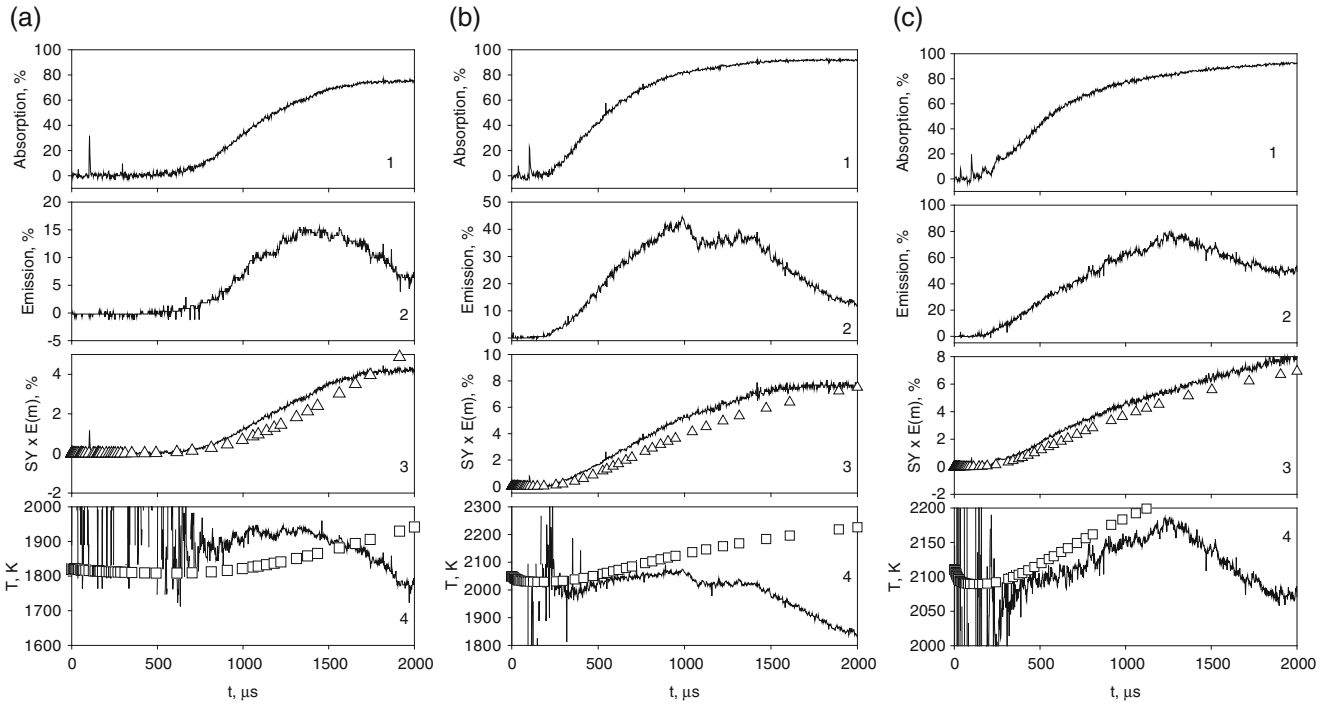

Fig. 1 Typical time histories of the absorption (1) and emission (2) signals after the arrival of the reflected shock wave front at the observation section and of the soot yield (3) and soot particles temperature (4) obtained from signals (1) and (2) for a 4.8 % mixture of acetylene in argon at various conditions behind the reflected shock wave: (**a**) $T_{50} = 1821$ K, $[M]_{50} = 2.36 \times 10^{-5}$ mol/cm^3, $P_{50} = 3.53$ bar; (**b**) $T_{50} = 2049$ K, $[M]_{50} = 1.93 \times 10^{-5}$ mol/cm^3, $P_{50} = 3.25$ bar; (**c**) $T_{50} = 2111$ K, $[M]_{50} = 2.32 \times 10^{-5}$ mol/cm^3, $P_{50} = 4.02$ bar. The probe light wavelength was $\lambda = 632.8$ nm. The points (*triangles* and *squares*) represent the calculated values of the soot yield and soot particles temperature, whereas the lines in panels 3 and 4 are the results of processing the experimental absorption (*curve 1*) and emission (*curve 2*) signals, respectively

(c) 2.5 % C_2H_2 + 7.5 % H_2 + 90.0 % Ar. The results for diacetylene are shown in Fig. 4: (a)–(d) the pyrolysis of three different C_4H_2/H_2/Ar mixtures (1.0 % C_4H_2 + 99.0 % Ar, 1.0%C_4H_2 + 1.0 % H_2 + 98.0 % Ar, 1.0 % C_4H_2 + 4.0 % H_2 + 95.0 % Ar) and (e)–(h) the oxidation of a 0.4 % C_4H_2 + 0.9 %O_2 + 98.7 %Ar mixture. As can be seen from Figs. 4 and 5, the calculated and experimentally measured values are in close agreement.

The kinetic model of soot nucleation used in our previous works, which was based on reactions of recombination of polyaromatic fragments, was supplemented by reactions of nucleation through the combination of C_8H_4 aliphatic dimers. This modification was motivated by the experimental results from [5, 8, 9], where these species were reliably detected.

It was concluded in [5] that the C_8H_4 excited isomer is a common intermediate for the formation of polyynes and oligomers, that higher polyynes cannot be formed in the direct reactions $C_4H_2 + C_2H_2 = C_6H_2 + H_2$ and $C_4H_2 + C_4H_2 = C_8H_2 + H_2$, and that the C_8H_4 linear isomers dissociate to C_8H_2, whereas branched C_8H_4 isomers react further to produce heavier oligomers or decompose to form C_6H_2 molecules. The addition of C_4H_2 to the C_8H_4 branched isomer is accompanied by cyclization into a species containing an aromatic ring, with the resulting product being capable of further polymerization. In this case, the larger the oligomers formed, the less likely is the formation of relatively stable condensed aromatic compounds with side chains.

In [9], the polyynic structures (polyynes and substituted derivatives thereof) were observed in fuel-rich low-pressure allene, propyne, and cyclopentene flames by using photoionization time-of-flight mass spectrometry with tunable vacuum-ultraviolet synchrotron radiation; in particular, a number of C_7H_4 and C_8H_4 isomers were detected.

In contrast to $C_{2n}H_2$ polyyne molecules, the possible reaction pathways that lead to the formation of the C_7H_4 and C_8H_4 isomers remain mostly unexplored. Probably, such reactions proceed through the formation of similar but smaller intermediates.

Our kinetic simulations were performed using the mechanism of soot formation developed in [4]. This mechanism of the formation of soot particles includes a submechanism of gas-phase reaction for describing the pyrolysis and oxidation of the starting hydrocarbons, in particular acetylene, and the formation and growth of polyaromatic hydrocarbon molecules through various channels, up to coronene.

The core of the gas-phase reaction mechanism is the reaction sequence of PAH formation in laminar premixed

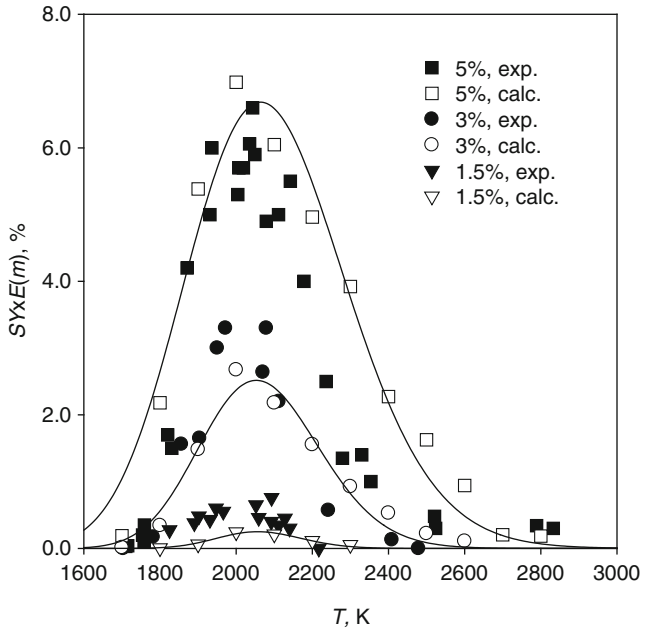

Fig. 2 Experimentally measured and calculated temperature dependences of the soot yield in the pyrolysis of three different acetylene–argon mixtures behind reflected shock wave: (*filled square*) 5 %, (*filled circle*) 3 %, and (*filled inverted triangle*) 1.5 % C_2H_2 in argon (P_{50} = 3.0–4.5 bar, $E(m)$ = 0.37, τ_{reac} = 1 ms). The closed symbols represent the results of experimental measurements; open symbols represent the results of detailed kinetic calculations, and lines represent the results of approximation of experimental values by a nonlinear regression (the left figure)

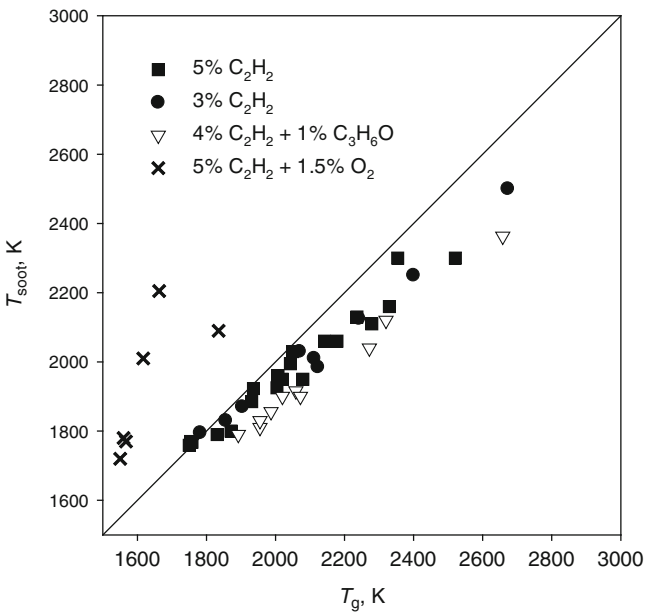

Fig. 3 Dependence of the temperature of soot particles formed in the pyrolysis of acetylene–argon mixtures for a time of τ_{reac} = 1 ms after shock heating of the mixture on the calculated initial temperature behind the reflected shock wave. The compositions of the mixtures are given in the figure panels, where C_3H_6O is acetone (the right figure)

acetylene and ethylene flames (HACA). At the same time, the mechanism was extended to include a number of additional channels of PAH formation and growth (up to coronene) and a comprehensive set of reactions involving C_3, C_5, and C_7 hydrocarbons. More specifically, the mechanism included (1) the alternating H-abstraction/C_2H_2-addition route, resulting in the successive growth of PAHs, (2) the combination reactions of phenyl with C_6H_6, (3) the cyclopentadienyl recombination, and (4) the ring-closure reactions of aliphatic hydrocarbons.

The principles of constructing this kinetic mechanism were outlined in [4]. The modified gas-phase reaction mechanism consisted of 3531 direct and inverse reactions involving 300 different components, with the rate constants of several important reactions being pressure dependent.

The processes of formation, growth, oxidation, and coagulation of soot particle nuclei and actually soot particles were simulated using the discrete Galerkin method [10].

According to our model, soot precursors are formed by radical–molecule reactions of different PAHs, starting from phenylacetylene, acenaphthylene, and ethynylnapthalene up to coronene, by radical–radical reactions (from cyclopentaphenanthrene up to coronene radicals), and by combination reactions of unsaturated polyyne-like aliphatic hydrocarbons C_8H_4. The reactions of formation of soot precursors are assumed irreversible. These reactions result in the formation of polyaromatic molecules containing 16–48 carbon atoms and reactive aliphatic oligomers, containing initially 16 carbon atoms. All these compounds grow further, being stabilized by the formation of new chemical bonds. Soot precursors are activated in reactions with H and OH radicals and deactivated in reactions with H, H_2, and H_2O. Soot precursors grow via reactions with C_2H_2, C_4H_2, and C_6H_2 (the concentrations of which are rather high in the pyrolysis and oxidation of aliphatic and aromatic hydrocarbons), reactions with polyaromatic molecules and radicals, and the process of coagulation. Soot precursors are oxidized by O and OH radicals. They are transformed into soot particles through internal conversion reactions, in which the number of active sites in the reacting system is preserved. Soot particles grow in the reactions with C_2H_2, C_4H_2, C_6H_2, and PAH molecules and radicals and are oxidized by O and OH radicals. All soot particles were postulated to participate in coagulation.

Since the temperature behind the reflected shock wave varies with time in a complicated way (rapid fall to a quasi-steady-state value, growth, and a new decrease upon the arrival of the rarefaction wave), the ultimate soot yield is determined by the entire temperature profile, not only by the quasi-steady-state temperature. Thus, all kinetic calculations were performed for nonisothermal conditions and a constant density, and the calculated kinetic data are in good agreement with the corresponding experimental data. For this

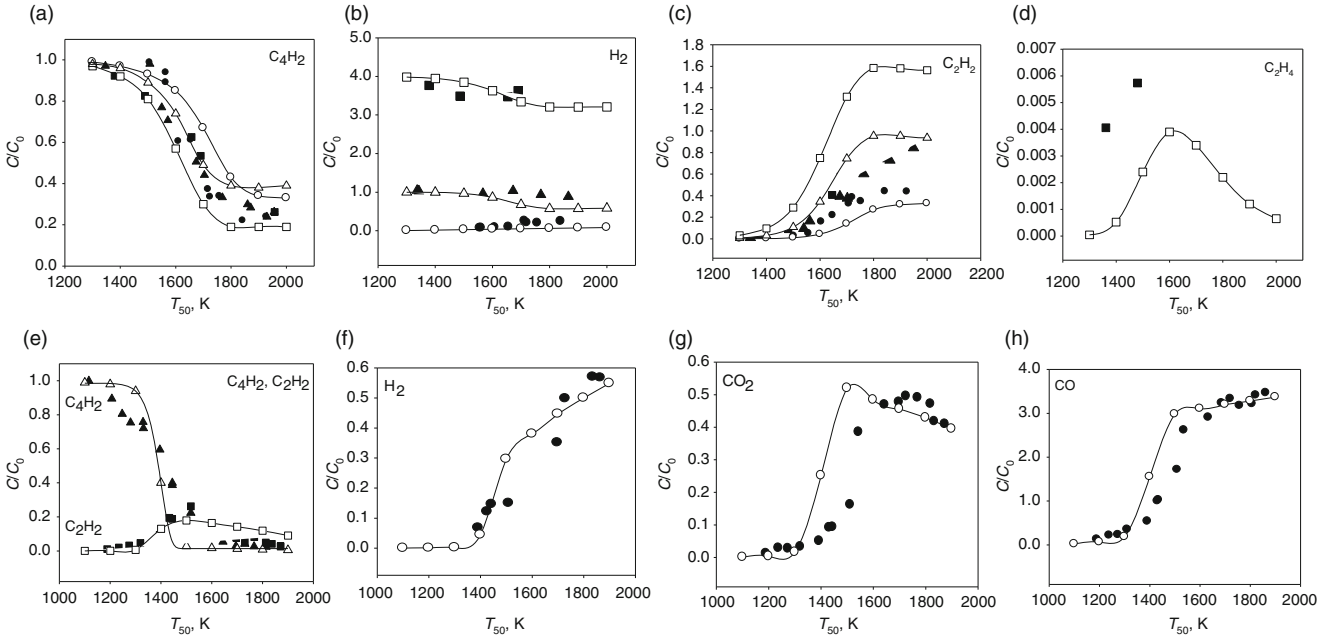

Fig. 4 Direct comparison of the experimentally measured (*closed symbols*) [6] and calculated (*open symbols*) product yields during (the *top row*) pyrolysis of three different C_4H_2/H_2 mixtures in Ar ((*filled circle*) 1.0%C_4H_2 + 99.0%Ar, (*filled inverted triangle*) 1.0% C_4H_2 + 1.0%H_2 + 98.0%Ar, and (*filled square*) 1.0%C_4H_2 + 4.0% H_2 + 95.0%Ar) and (the *bottom row*) oxidation of a 0.4% C_4H_2 + 0.9%O_2 + 98.7%Ar mixture. The reaction time τ_{react} was varied with the initial temperature T_{50} behind the reflected shock wave by exactly the same way as presented in [6]; C/C_0 means the ratio of the corresponding product concentration and the initial C_4H_2 concentration in a particular experiment or calculation

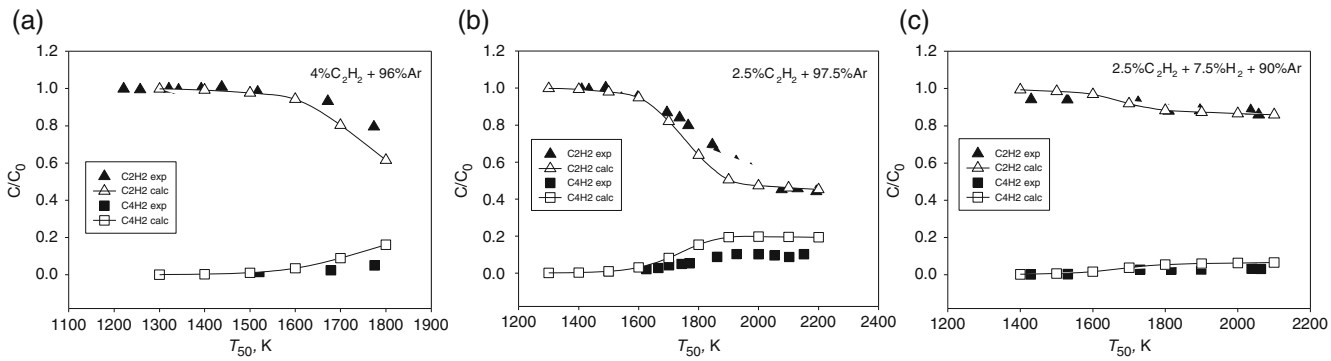

Fig. 5 Comparison of the experimentally measured [7] (*closed symbols*) and calculated (*open symbols*) product yields for the pyrolysis of various C_2H_2/H_2/Ar mixtures: (**a**) 4.0%C_2H_2 + 96%Ar, (**b**) 2.5% C_2H_2 + 97.5%Ar, (**c**) 2.5%C_2H_2 + 7.5%H_2 + 90.0%Ar. The reaction time τ_{react} was varied with the initial temperature T_{50} behind the reflected shock wave in the exactly same way as described in [7]; C/C_0 is the ratio of the corresponding product concentration and the initial C_2H_2 concentration in a particular experiment or calculation

reason, we did not adjust our experimental data points to some "effective temperature" behind the reflected shock wave and used the initial temperature T_{50} both in the representation of experimental data and in the calculations.

Introduction into the soot formation kinetic model of the soot nuclei produced from unsaturated aliphatic hydrocarbons, along with those arising from polyaromatic compounds, makes it possible to significantly improve the kinetic description of the experimental time histories of soot formation (Fig. 1) and temperature and concentration dependences of the soot yield (Fig. 2) not only for acetylene pyrolysis but for pyrolysis and oxidation of all aliphatic and aromatic hydrocarbons being investigated. The proposed kinetic model of soot formation correctly predicts the location of the maximum in the temperature dependences of the soot yield for all hydrocarbons studied, including C_2H_2/Ar mixtures. Within the scatter in experimental values of the soot yield, the model predictions of this quantity obtained

using a fixed value of $E(m) = 0.37$ for all hydrocarbons investigated are in good agreement with our experiments.

Since there is a considerable discrepancies between the reported values of $E(m)$, we plotted the quantity $SY \times E(m)$ as a function of the time and the initial shocked-gas temperature T_{50}. Studying the formation of soot during the pyrolysis of toluene behind reflected shock waves [1], we estimated $E(m)$ as 0.37, a value in close agreement with most recent data [11, 12]: according to [11], $E(m) = 0.373$, whereas in [12], $E(m) = 0.259$. The quantity $E(m) = 0.37$ has the advantage of being determined under conditions similar to those used in the present experiments.

Prior to the appearance of soot particles, the signal-to-noise ratio is too low to reliably determine the soot particle temperature. After the arrival of the rarefaction wave to the observation section (~1100–1500 μs), the emission signal begins to decrease markedly, indicative of a decrease in the mixture temperature in this cross section. The formal procedures and details of soot yield determination and measuring the soot particle temperature are presented in [1].

Conclusions

The experiments on the pyrolysis and oxidation under fuel-rich conditions of C_2H_2/Ar, C_2H_6/Ar, C_2H_4/Ar, C_2H_4/O_2/Ar, CH_4/Ar, CH_4/O_2/Ar, C_3H_8/Ar, C_3H_6/Ar, toluene/Ar, and benzene/Ar mixtures behind reflected shock waves were performed. The soot yield and the soot particle temperature were determined using the double-beam absorption-emission technique. Our experiments demonstrated that the soot formation in the pyrolysis of all aliphatic and aromatic hydrocarbons tested except for acetylene is accompanied by a pronounced temperature decrease due to the predominance of endothermic decomposition stages. In the case of acetylene pyrolysis, the temperature remains nearly constant, as it does in the oxidation of rich hydrocarbon/oxygen mixtures due to exothermic oxidation reactions. By contrast, a sharp and pronounced temperature increase is observed in the oxidation of rich acetylene/oxygen mixtures. Our previous kinetic model of soot formation during the shock-tube pyrolysis and oxidation of aliphatic and aromatic hydrocarbons is augmented by introducing an additional subset of reactions of soot nucleation, involving both polyaromatic and unsaturated aliphatic hydrocarbons. The proposed kinetic model was successfully tested by describing the published data on the products yield in the pyrolysis and oxidation of acetylene and diacetylene in shock-tube experiments. It closely reproduces our experimental data on the time histories of the soot yield and soot particle temperature, as well as the temperature and concentration dependences of the soot yield at fixed reaction times, for the pyrolysis and oxidation of C_2H_2/Ar, C_2H_6/Ar, C_2H_4/Ar, C_2H_4/O_2/Ar, CH_4/Ar, CH_4/O_2/Ar, C_3H_8/Ar, C_3H_6/Ar, toluene/Ar, and benzene/Ar mixtures under fuel-rich conditions in reflected shock waves ($T_{50} = 1400$–2850 K, $P_{50} = 2.5$–5.5 bar).

References

1. Agafonov, G.L., Smirnov, V.N., Vlasov, P.A.: Soot formation in the pyrolysis of benzene, methylbenzene, and ethylbenzene in shock waves. Kinet. Catal. **52**(3), 358–370 (2011)
2. Agafonov, G.L., Borisov, A.A., Smirnov, V.N., Troshin, K.Y., Vlasov, P.A., Warnatz, J.: Soot formation during pyrolysis of methane and rich methane/oxygen mixtures behind reflected shock waves. Combust. Sci. Technol. **180**(10), 1876–1899 (2008)
3. Agafonov, G.L., Smirnov, V.N., Vlasov, P.A.: Shock tube and modeling study of soot formation during pyrolysis of propane, propane/toluene and rich propane/oxygen mixtures. Combust. Sci. Technol. **182**(11), 1645–1671 (2010)
4. Agafonov, G.L., Smirnov, V.N., Vlasov, P.A.: Shock tube and modeling study of soot formation during the pyrolysis and oxidation of a number of aliphatic and aromatic hydrocarbons. Proc. Combust. Inst. **33**, 625–632 (2011)
5. Homann, K.H., Pidoll, U.: The low-pressure pyrolysis of butadiyne (C_4H_2). Ber. Bunsenges. Phys. Chem. **90**, 847–854 (1986)
6. Hidaka, Y., Henmi, Y., Ohonishi, T., Okuno, T., Koike, T.: Shock-tube and modeling study of diacetylene pyrolysis and oxidation. Combust. Flame. **130**, 62–82 (2002)
7. Hidaka, Y., Hattori, K., Okuno, T., Inami, K., Abe, T., Koike, T.: Shock-tube and modeling study of acetylene pyrolysis and oxidation. Combust. Flame. **107**, 401–417 (1996)
8. Homann, K.H.: Formation of large molecules, particulates and ions in premixed hydrocarbon flames; progress and unresolved questions. Proc. Combust. Inst. **20**, 857–870 (1984)
9. Hansen, N., Klippenstein, S.J., Westmoreland, P.R., Kasper, T., Kohse-Höinghaus, K., Wang, J., Cool, T.A.: A combined ab initio and photoionization mass spectrometric study of polyynes in fuel-rich flames. Phys. Chem. Chem. Phys. **10**, 366–374 (2008)
10. Deuflhard, P., Wulkow, M.: Computational treatment of polyreaction kinetics by orthogonal polynomials of a discrete variable. Impact Comput. Sci. Eng. **1**, 269–301 (1989)
11. Williams, T.C., Shaddix, C.R., Jensen, K.A., Suo-Anttila, J.M.: Measurement of the dimensionless extinction coefficient of soot within laminar diffusion flames. Int. J. Heat Mass Transfer. **50**, 1616–1630 (2007)
12. Smyth, K.C., Shaddix, C.R.: The elusive history of m = 1.57 – 0.56i for the refractive index of soot. Combust. Flame. **107**, 314–320 (1996)